Proceedings of the 28th IEEE
EMBS Annual International Conference
New York City, USA, Aug 30-Sept 3, 2006

Skin Penetration of Silicon Dioxide Microneedle Arrays

Sangchae Kim, Smitha Shetty, Dorielle Price, and Shekhar Bhansali*

BioMEMS and Microsystems Laboratory, Department of Electrical Engineering,
University of South Florida, 4202 E.Fowler Ave. ENB 118, Tampa, FL 33620
bhansali@eng.usf.edu, Tel: (813) 974-3593, Fax: (813) 974-5250

Abstract— **Out-of-plane hollow silicon dioxide microneedle arrays were fabricated and investigated to determine their efficacy for transdermal applications. The fabrication process of the SiO_2 microneedles is described, and mechanical fracture forces were investigated on microneedles with different geometrical dimensions. Biomechanical characterization of the microneedles was performed to specifically test for reliable stratum corneum and skin insertion by changing the regulatory parameters such as needle width and cross-section.**

Index Terms— **Microneedle, Skin, Stratum Corneum, MEMS**

I. Introduction

Microneedles are emerging as critical enhancers in transdermal drug delivery and fluid extraction systems owing to advances in micro fabrication technology and scalability into a multi-array configuration [1, 2]. Topical administration provides a large surface absorption area and negligible enzymatic degradation, thus overcoming limitations of oral treatment. As compared to commercially available hypodermic needles, microneedles enable pain free insertion, minimal tissue damage and increased control over drug dosage, independent of drug composition and concentration [1, 3]. To accelerate their inclusion into mainstream medicine and to advance their applicability, microneedles need to conform to requirements of simple design, low cost, mass production and reliability. While past research has focused on optimizing design and cost factors, performance studies specific for biomedical applications have so far been inadequate. Stratum Corneum (SC), the tough outermost barrier of the skin is approximately a 10-20 micron thick matrix of keratinized corneocyte cells embedded in a lipid rich intracellular space and interconnected by protein rich rivets "corneodesmosomes". It is necessary to investigate the biomechanical reaction at both the stratum corneum alone and the entire composition of skin (epidermis and dermis).

This research intends to address this issue by quantitatively characterizing reliability with respect to the stratum corneum and the whole skin with respect to dimensional variations of microneedles via fracture and cadaver skin penetration tests. The micromachining approaches using deep reactive ion etching (DRIE) was implemented to fabricate biocompatible microneedle arrays. Robust needle configurations would facilitate development of implantable needle arrays for continuous body monitoring for diseased conditions, like diabetes, without susceptibility to body corrosion as observed in metallic needles.

II. Fabrication

Microneedle fabrication was based on a bulk machining process to obtain straight walled pores of varying depths by using DRIE (dry process). Parametric investigation was feasible from DRIE based microneedles since different patterns could be lithographically fabricated with ease on a single wafer. Figure 1 shows the fabrication process for the SiO_2 microneedle arrays. A 4-inch single side polished wafer is prepared and cleaned. Al (3000Å) was evaporated as a masking layer for the DRIE silicon etching process. S-1818 positive photoresist was patterned and Al was etched using Al wet etchant. The exposed Si surface was subjected to 400 Bosch cycles using the DRIE machine to make deep straight holes at predetermined microneedle lengths. Once the pores were defined, the Al etching mask was fully removed and the wafer was oxidized in the thermal furnace up to 1.5 μm, which is the wall thickness of the microneedles. Next the wafer was lapped to open the backside of holes and diced into individual chips. Then the diced chips were subjected to a time controlled Si wet etch, resulting in hollow SiO_2 needles. Figure 2 shows the SEM images of the fabricated microneedle array.

III. Experimental Setup

The experimental setup for mechanical fracture test and skin (or stratum corneum) penetration test was designed to house two basic modules: needle attachment block and bio sample (skin or stratum corneum) loading block. They were positioned horizontally to face each other. The reaction force between the microneedles and bio sample was measured using a sensitive tension-compression load cell (LCFA-500 gF sensing capacity, Omega Co.) attached to the bio-sample mounting fixture. The load cell was interfaced to one channel load cell input, 16-Bit, RS-485 data acquisition module (Superlogics-8016) to obtain real time results. The needle attachment block (0.9cm×0.9cm microneedle chip mounted on steel block) was supported on XYZ stage and was driven by 0.1 μm resolution differential micrometers. Real time image capture capability on probe station facilitated in the

determination of instant needle insertion. The bio-samples were mounted on a 2cm×4cm Teflon block using an adhesive.

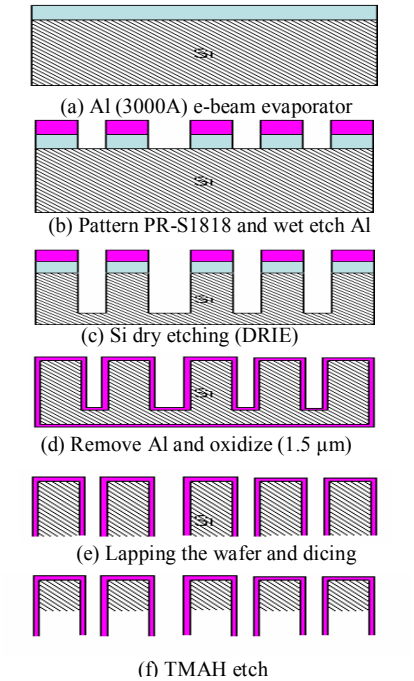

Fig. 1. Fabrication process for SiO2 microneedles

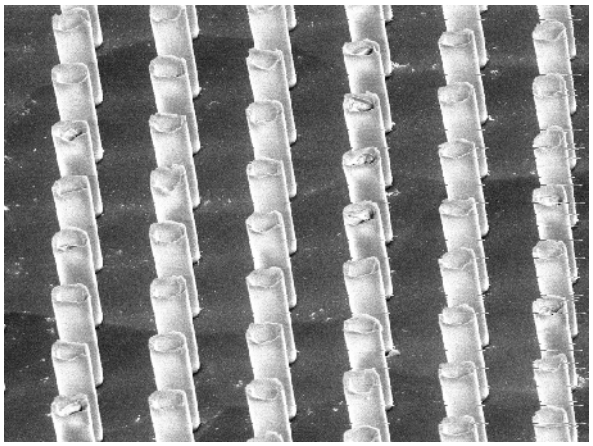

Fig. 2. Scanning electron microscope illustration of fabricated microneedle array (5 μm diameter, 20 μm pitch)

IV. Mechanical Fracture Test

In-plane fracture tests were performed on one microneedle to observe the effect of needle geometry on fracture force. The axial force required to fracture a silicon dioxide needle column was experimentally measured by compressing the chip at rate of 1 μm/sec against the load cell mounting plane. The point of fracture was visually captured by the camera together with the data acquisition system displaying a sharp peak in the force-time graph, interpreted as the needle failure point. Once this peak was achieved, the needles were retracted at the same rate.

Figure 3 is a typical plot of the force on the needle vs. time for a square needle with length 125 μm and width 40 μm with the peak representing the maximum force (2.33 gF) applied to needle before failure. The point of fracture is denoted by the outlier shown in Figure 3. The rise and fall of the peak changes abruptly because the instant of fracture is very short and the sampling time is 1 second. The sudden drop after the peak indicates that the needle and load cell are no longer in contact. The geometrical testing results were investigated for varying widths and lengths. The observed readings did not obey the inverse parabolic relation between force and length given by analytical values in accordance to Euler's buckling relation for long slender columns. However as expected, the fracture force decreased with increasing length. Small fractures in SiO_2 can be attributed to microscopic crack defects in the structure leading to crack initiation and propagation [4]. This stress concentration could have magnified the stresses at the crack tip, and these cracks grew much more quickly, thus causing the material to fracture long before it ever reached its theoretical strength.

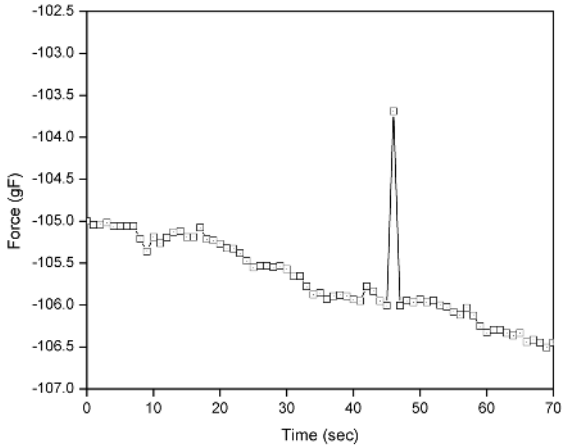

Fig. 3. Reaction force variation of a square needle with length 125 μm and width 40 μm

V. Preparation of Skin Samples

Skin samples were prepared on 1cm×1cm excised split-thickness skin specimens obtained from the U.S. Cell and Tissue Bank in Ohio. Room temperature (70-73 ^{0}F) and humidity (40%) were kept constant throughout the experimentation. The cryo-preserved samples were thawed to room temperature and were observed to dehydrate fast. The hydration issue related to the skin was resolved by applying physiological saline every 5 minutes. Excess water from the stratum corneum surface was wiped to ensure close to 100% humidity for the skin samples. Each chip was observed under an optical microscope before each experiment to verify the overall needle integrity. SEM images of the needles were obtained to observe the condition of the needles after penetration.

VI. Penetration of Stratum Corneum

The ability of the microneedles to penetrate enzymatically isolated stratum corneum was put to test. A stratum corneum specimen placed on soft polymer was mounted on the skin holding block and subjected to insertion of an India ink stained microneedle array (25×25 square needle array-width 40 μm, pitch 150 μm, length 100 μm) for penetration force quantification. The needle insertion was done using a manual micrometer with an insertion rate of 10–20 μm. Also the plots exhibited several non uniformities due to uneven microneedle motion as shown in Figure 4. The test results which exhibited sharp penetration peaks have been summarized in Table I. The graphs as well as the images indicate possible penetration into stratum corneum. The large force values are due to dehydration of stratum corneum, transforming into a hard material.

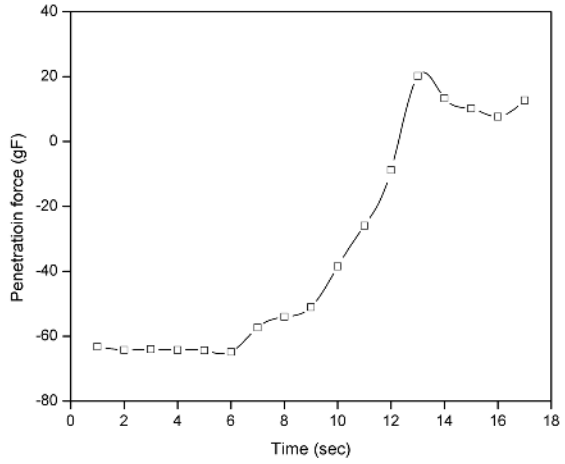

Fig. 4. Stratum corneum penetration plot for 25×25 microneedle array ((square, needle-width 40 μm, pitch 150 μm, length 100 μm)

TABLE I
STRATUM CORNEUM PENETRATION OF MICRONEEDLE ARRAYS

specifications		width (μm)	pitch (μm)	length (μm)	Penetrat-i on force (gF)
Array	cross-sec tion				
25×25	square	40	150	100	84.68
25×25	square	40	100	100	77.05

Penetration experiments provide an approximate quantitative analysis for the insertion force into split thickness and stratum corneum despite specimen surface morphology. The needles were found to be mechanically sturdy enough to insert into the skin without fracture. As compared to force requirements for metal and polymer microneedles (8-300 gF/needle) [5, 6], SiO_2 needle arrays required very small forces of the order of tens of gF for effective penetration.

VII. Penetration of Whole Skin

Skin penetration experiments were done using motorized micrometer with insertion rate of 50 μm/sec. These results were found to be encouraging since some results exhibited a sharp peak indicating possible stratum corneum insertion with similar India ink dye marks. A sample penetration plot has been shown in Figure 5 for a 25×25 needle array (needle width 60 μm, pitch150 μm, length 105 μm) with force peak of 4.03 gF. The results from the penetration tests have been summarized in Table II. The table also shows that several tests did not display a sharp penetration peak, thereby leading to non quantification of force values. This inability could be attributed to the following factors: rough nature of skin at microscopic level or non uniform microneedle edges. Since the cadaver specimens exhibited high surface roughness, all needles must not have penetrated at the same instant; hence the point loading may be significantly higher than the read out values.

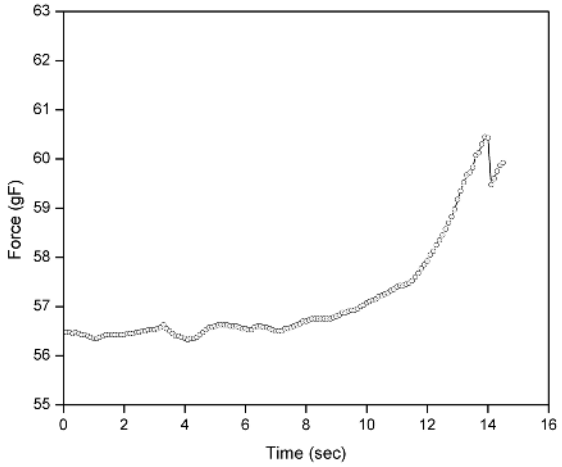

Fig. 5. Typical skin penetration force-time plot for 25×25 array (circular, needle-width 60 μm, pitch 150μm, length 105 μm). The peak indicates the penetration force required for insertion

TABLE II
SPLIT THICKNESS PENETRATION RESULTS USING MOTORIZED MICROMETER

Microneedle specifications		width (μm)	pitch (μm)	length (μm)	Penetration force (gF)
array	Cross-section				
5×5	circular	40	100	100	8.10
5×5	circular-repeat	40	100	100	0.23
5×5	square	20	150	90	No peak
5×5	circular	20	200	110	0.13
5×5	square	40	200	100	0.15
5×5	circular	40	200	95	No peak
5×5	circular	60	200	100	No peak

25×25	circular	20	100	95	No peak
25×25	square	20	100	95	0.13
25×25	circular	40	200	110	2.18
25×25	square	40	200	150	2 peaks - 0.28 & 1.98
25×25	circular	60	150	105	4.03
25×25	circular-repeat	60	150	105	2 peaks - 1.63 & 3.15
25×25	square- on different location	40	200	110	No peak

During insertion testing, it was crucial to confirm that the needles actually penetrate through the corneocytes as against surface indentation. Though the black India ink marks and cutting peaks observed in force plots for some needle configurations were useful evidences favoring skin penetration, it was necessary to determine the penetration depth through sectioning. Observations using an optical microscope showed, some sections demonstrated 60~90 µm deep and 20 µm wide penetration marks into the epidermis layer as illustrated in Figure 6. However the intra-array pitch was observed to be approximately 50 µm as against 100 µm. Multiple insertions during skin fixation along with non-uniform sections due to skin wrinkling could account for this irregularity. Also, Figure 7 illustrates the black ink marks on a skin specimen after an insertion test.

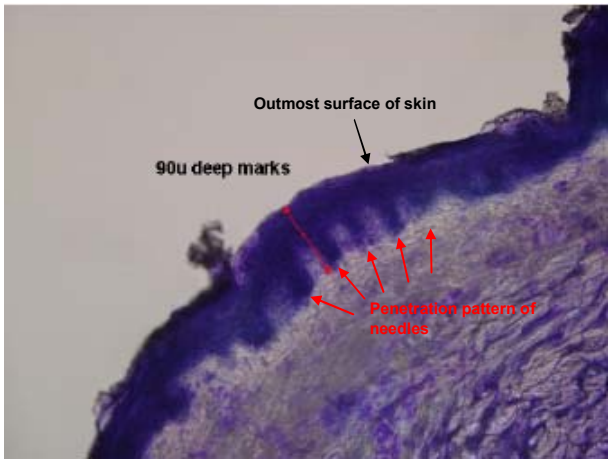

Fig. 6. Microscope image (4X magnification) illustrating microneedle penetration marks

VIII. Conclusion

Out-of-plane SiO_2 microneedle arrays were fabricated using bulk Si micromachining techniques with different shapes and dimensions. An experimental setup was developed for fracture and skin penetration force measurements. Microneedle reliability was quantified experimentally. Real time microneedle insertion tests into cadaver skin and isolated stratum corneum experimentally highlighted the robustness of the needles to penetrate without fracture. The penetration force required for a 25×25 array was on the order of 1~5 gF as compared to 0.25 ~ 0.7 gF for a 5×5 array. Experimental characterization confirmed mechanical robustness of SiO_2 microneedles for transdermal applications.

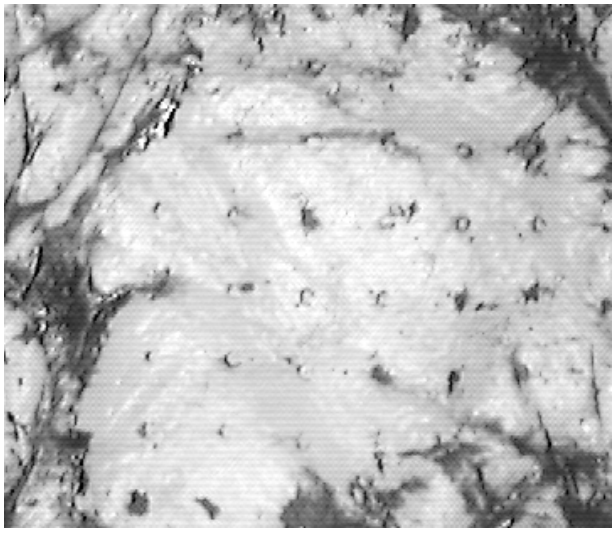

Fig. 7. Optical microscope image illustrating black India ink stains on cadaver skin after insertion of 25×25 array with square needles (width 40 µm, pitch 200 µm, and height 125 µm)

References

[1] S. P. Davis, B. J. Landis, Z. H. Adams, M. G. Allen, M. R. Prausnitz, Journal of Biomechanics, Vol. 37, No. 8, pp.1155-1163, 2004.

[2] Zahn, Talbot, Leipmann and Pisano, Biomedical Microdevices, Vol. 2, pp.295-303, 2000.

[3] S. Chandrasekaran and B. Frazier, Journal of Microelectromechanical systems, Vol. 12, No. 3, pp. 289-295, 2003.

[4] Lawn B., "Fracture of brittle solids", Cambridge University Press, 1993.

[5] Gardeniers H., Luttge R., Berenschot E., Boer M., Yeshurun S., Hefetz M., Oever R. and Berg A., "Silicon Micromechanical Hollow Microneedles for Transdermal Liquid Transport", Journal of Microelectromechanical systems, Vol. 12, 6, pp. 855-862, Dec. 2003.

[6] Griss P. and Stemme G., "Side-Opened Out-of-Plane Microneedles for Microfluidic Transdermal Liquid Transfer", Journal of Microelectromechanical systems, Vol. 12, 3, pp. 296-301, June 2003.

Acknowledgements

This research is partially funded by NSF awards 0239262and 0630110 and USAMRMC with the title of "Cardiovascular Battlefield Injury Diagnostic & Treatment Sensor & MEMS Technology Development". Dorielle Price is supported through NSF and Ford foundation Graduate Fellowships.